

Ohmic heating – asymmetry of flow due to natural convection

Žitný R., CTU in Prague, FME, October 2000

Keywords: Ohmic heating, parallel flows, natural convection

1. Introduction

It was observed experimentally that the parallel flows in lateral channels of continuous ohmic heaters are symmetric only at isothermal conditions. In case of heating, one stream is delayed and even stopped or reversed if the temperature increase is too high. This phenomenon can be explained by natural convection, see Fig.1.

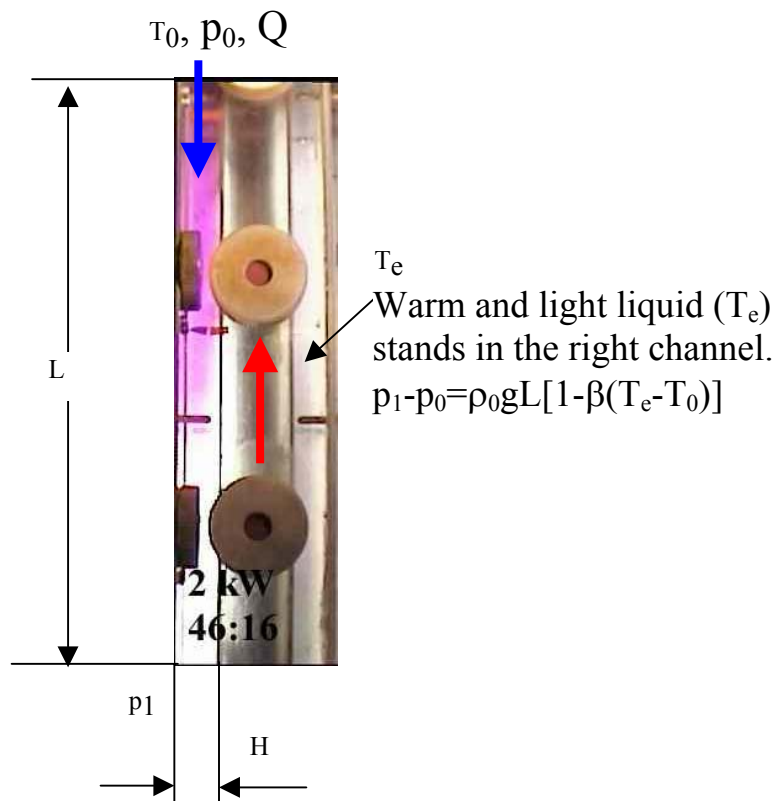


Fig.1

2. Analysis of the case when liquid flows only in one channel

The analysis is based upon the fact that the pressure difference $p_1 - p_0$ is the same in the left and in the right channel.

$$p_1 - p_0|_{left} = \rho_0 g L [1 - \beta(\bar{T}_1 - T_0)] - L f \bar{u}$$

$$p_1 - p_0|_{right} = \rho_0 g L [1 - \beta(T_e - T_0)] \tag{1}$$

$$\rho_0 g \beta (\bar{T}_1 - T_e) = -f \bar{u}$$

where (see e.g. Novak 1989)

$$f = \frac{12\mu}{H^2(1 - \frac{192H}{\pi^5 B} \sum_{n=1,3,5,\dots} \frac{1}{n^5} \operatorname{tgh} \frac{n\pi B}{2H})} \quad \text{and} \quad \bar{u} = \frac{Q}{HB} \quad (2)$$

The temperature course $T(x)$ in the left channel can be estimated from the heat balance

$$\rho_0 c_p \bar{u} B H (T - T_0) = \alpha_{\ln} B L \frac{T - T_0}{\ln \frac{T_e - T_0}{T_e - T}}$$

$$\text{giving } T_e - T = (T_e - T_0) \exp\left[-\frac{\alpha_{\ln} x}{\rho_0 c_p \bar{u} H}\right] \quad (3)$$

and the mean temperature in the left channel is therefore

$$T_e - \bar{T}_1 = (T_e - T_0) \frac{1}{L} \int_0^L \exp\left(-\frac{\alpha_{\ln} x}{\rho_0 c_p \bar{u} H}\right) dx = (T_e - T_0) \frac{\rho_0 c_p \bar{u} H}{\alpha_{\ln} L} \left[1 - \exp\left(-\frac{\alpha_{\ln} L}{\rho_0 c_p \bar{u} H}\right)\right] \quad (4)$$

Substituting Eq.(4) into Eq. (1) follows

$$T_e - T_0|_{\text{stability}} = \frac{12\mu\alpha_{\ln} L}{H^3 g \beta \rho_0^2 c_p \left[1 - \exp\left(-\frac{\alpha_{\ln} L}{\rho_0 c_p \bar{u} H}\right)\right] \left(1 - \frac{192H}{\pi^5 B} \sum_{n=1,3,5,\dots} \frac{1}{n^5} \operatorname{tgh} \frac{n\pi B}{2H}\right)} \quad (5)$$

and this is the final relationship, valid under assumptions

- Temperature of electrodes is a constant
- Flow is laminar
- Heat transfer coefficient is a constant

Example of results, presented in Fig.2, follows from simplified equation corresponding to the first three terms of exponential term expansion in Eq.(5)

$$T_e - T_0|_{\text{stability}} = \frac{12\mu Q}{H^3 B g \beta \rho_0 \left[1 - \frac{Nu_{\ln} La \left(\frac{B}{H} + 1\right)}{4Q}\right] \left(1 - \frac{192H}{\pi^5 B} \sum_{n=1,3,5,\dots} \frac{1}{n^5} \operatorname{tgh} \frac{n\pi B}{2H}\right)} \quad (6)$$

A constant Nu_{\ln} has been assumed and its numerical value was estimated according to Kays 1993, for the following parameters

$$B/H=6 \quad x^*=0.02 \quad D_h = \frac{2BH}{B+H}; \quad Re = \frac{\bar{u} D_h \rho_0}{\mu}; \quad Pr = \frac{\nu}{a}$$

$Nu_{\ln} = \alpha_{\ln} D_h / \lambda$	$x^* = 2L / (D_h Re Pr)$
10	0.01
8	0.02
6	0.1
5.22	>>1

ρ	β	μ	a	Q	H	B
kg/m ³	1/K	Pa.s	m ² /s	m ³ /s	m	m
1000	0.5e-3	0.6e-3	0.15e-6	50e-6	0.01	0.08

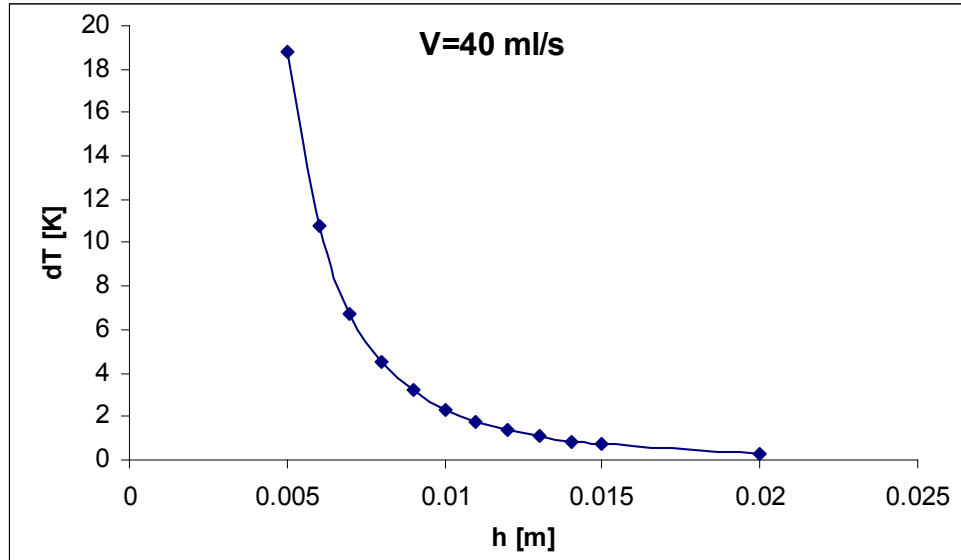


Fig.2

3. General case - liquid flows in both channels with different flowrate

This case can be analysed in exactly the same way as the preceding one. The requirement of the same pressure differences in channels leads to

$$\rho_0 g \beta (\bar{T}_2 - \bar{T}_1) = \frac{f}{BH} (2Q_1 - Q) \quad (7)$$

where Q_1 and Q are flowrate in the left and both channels respectively. Estimating mean temperature in channels according to Eq.(4) the final equation between temperature difference $T_e - T_0$ and flowrate Q_1 can be derived

$$T_e - T_0 = \frac{6\mu(2\psi - 1)La(1 + \frac{B}{H})}{H^3 g \beta \rho_0 B \left\{ \frac{\psi}{Nu_1} \left[1 - \exp\left(-\frac{aL Nu_1 (1 + \frac{B}{H})}{2Q\psi}\right) \right] - \frac{1-\psi}{Nu_2} \left[1 - \exp\left(-\frac{aL Nu_2 (1 + \frac{B}{H})}{2Q(1-\psi)}\right) \right] \right\} \left(1 - \frac{192H}{\pi^5 B} \sum_{n=1,3,5,\dots} \frac{1}{n^5} \operatorname{tgh} \frac{n\pi B}{2H} \right)} \quad (8)$$

where

$\psi = \frac{Q_1}{Q}$ is the relative flowrate in channel 1, and Nu_i is the mean Nusselt number in the i -th channel.

The Eq.(8) can be rewritten into dimensionless form

$$Ra = \frac{6(2\psi - 1) \frac{L}{B} (1 + \frac{B}{H})}{\left\{ \frac{\psi}{Nu_1} [1 - \exp(-\frac{L Nu_1}{H \psi Re Pr})] - \frac{1 - \psi}{Nu_2} [1 - \exp(-\frac{L Nu_2}{H(1 - \psi) Re Pr})] \right\} (1 - \frac{192H}{\pi^5 B} \sum_{n=1,3,5,\dots} \frac{1}{n^5} \operatorname{tgh} \frac{n\pi B}{2H})}$$

(9)

where

$Ra = \frac{g\beta(T_e - T_0)H^3}{av}$ and $Re = \frac{uD_h\rho}{\mu} = \frac{2Q}{v(H+B)}$ are Rayleigh and Reynolds numbers respectively.

4. Perforated electrodes natural convection considered in both channels

Continuous heater with perforated electrodes exhibits also rather complicated behaviour; because cross flow through perforation is a decreasing function of heating power. The reason can be also found in natural convection effects. Geometry of two lateral channels (denoted by indices l,r) and central channel (c) is shown in Fig.3.

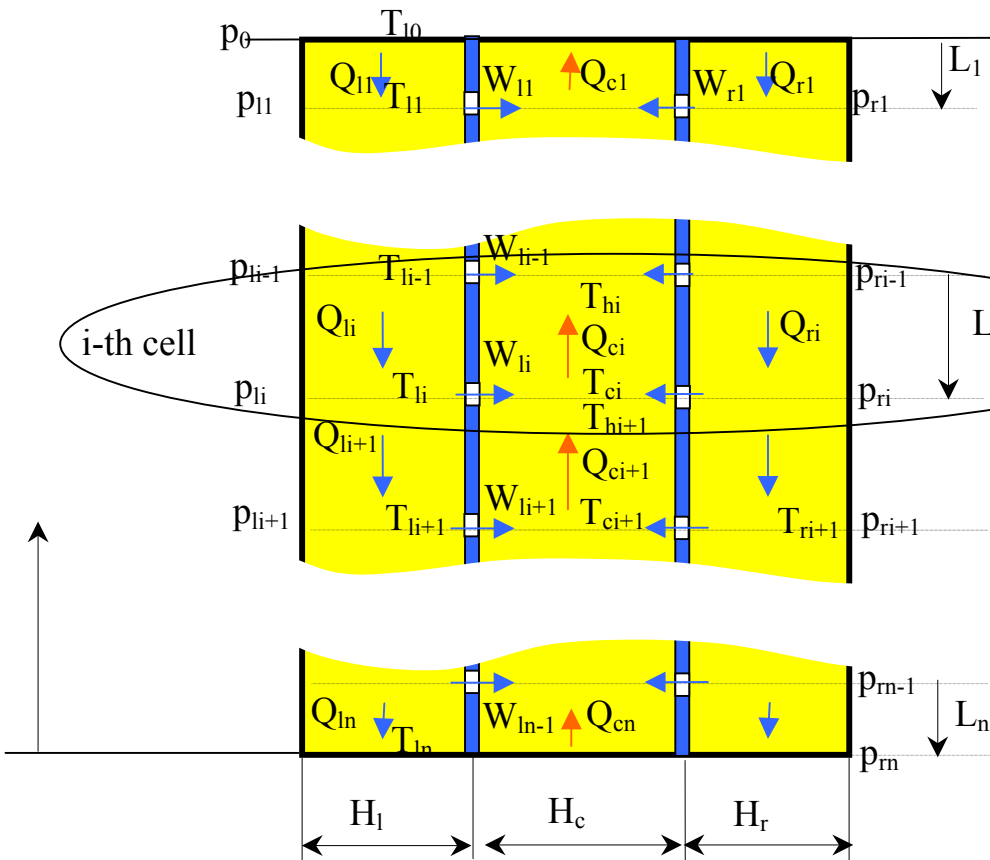


Fig.3
Integral model

The following analysis is based upon integral balances of control volumes formed by sections of heater between slits. It is assumed, that the flow inside these volumes is fully developed, laminar and in axial direction.

Continuity equation can be written for each cell inside lateral channels

$$Q_{li} = Q_{l0} - \sum_{j=1}^{i-1} W_{lj} \quad Q_{ri} = Q_{r0} - \sum_{j=1}^{i-1} W_{rj} \quad i=1,2,\dots,n \quad (10)$$

and for the central channel

$$Q_{ci} = Q_{li} + Q_{ri} = Q_{l0} + Q_{r0} - \sum_{j=1}^{i-1} (W_{lj} + W_{rj}) \quad i=1,2,\dots,n \quad (11)$$

Heat balance enables to estimate temperatures within the cells. Axial temperature profiles in lateral channels are assumed continuous, while the axial temperature profile are characterised by steps corresponding to injection of colder liquid in places where electrodes are perforated. The heater is assumed to be thermally insulated therefore the balances of enthalpy in lateral channels give

$$\rho c_p Q_{li} (T_{li} - T_{li-1}) = \frac{\alpha_l L_i B}{2} (T_{ci} + T_{hi} - T_{li} - T_{li-1}) \quad (12)$$

$$\rho c_p Q_{ri} (T_{ri} - T_{ri-1}) = \frac{\alpha_r L_i B}{2} (T_{ci} + T_{hi} - T_{ri} - T_{ri-1}). \quad (13)$$

Nevertheless, stability problems forced us to use fully implicit form of (12-13)

$$\rho c_p Q_{li} (T_{li} - T_{li-1}) = \alpha_l L_i B (T_{ci} - T_{li}) \quad (12a)$$

$$\rho c_p Q_{ri} (T_{ri} - T_{ri-1}) = \alpha_r L_i B (T_{ci} - T_{ri}) \quad (13a)$$

The axial temperature profile in the central channel is described by the step change at the interface between control volumes (mixing with lateral streams)

$$Q_{ci} T_{ci} - Q_{ci+1} T_{hi+1} = W_{li} T_{li} + W_{ri} T_{ri} \quad (14)$$

while the temperature change inside the cell is given by

$$\rho c_p Q_{ci} (T_{hi} - T_{ci}) = L_i B \left[-\frac{\alpha_l}{2} (T_{ci} + T_{hi} - T_{li} - T_{li-1}) - \frac{\alpha_r}{2} (T_{ci} + T_{hi} - T_{ri} - T_{ri-1}) + \kappa_i \frac{\Delta U^2}{H_c} \right] \quad (15)$$

Remark: Temperature T_{cn} at the bottom of heater is given by mixing streams from lateral channels

$$Q_{cn} T_{cn} = Q_{ln} T_{ln} + Q_{rn} T_{rn} \quad (14a)$$

Pressure distribution is determined by pressure losses and by gravity. Pressure losses can be calculated using the same method as previously, giving axial profiles of pressure in lateral channels

$$p_{li} - p_{li-1} = \rho_0 g L_i \left[1 - \beta \left(\frac{T_{li-1} + T_{li}}{2} - T_0 \right) \right] - L_i f_l Q_{li} \quad i=1,2,\dots,n \quad (16)$$

$$p_{ri} - p_{ri-1} = \rho_0 g L_i [1 - \beta(\frac{T_{ri-1} + T_{ri}}{2} - T_0)] - L_i f_r Q_{ri} \quad (17)$$

and in central channel

$$p_{ci} - p_{ci-1} = \rho_0 g L_i [1 - \beta(\frac{T_{ci} + T_{hi}}{2} - T_0)] + L_i f_c Q_{ci} \quad (18)$$

Friction coefficients in rectangular channels is given by

$$f_c = \frac{12\mu}{BH_c^3 (1 - \frac{192H_c}{\pi^5 B} \sum_{n=1,3,5,\dots} \frac{1}{n^5} \operatorname{tgh} \frac{n\pi B}{2H_c})} \quad (19)$$

Combining continuity equation with Eqs.(16-17) we can eliminate internal pressures and express the pressure at an arbitrary cell in terms of pressure at inlet and volumetric flowrate at inlet

$$p_{li} - p_0 = \sum_{j=1}^i \{ \rho_0 g L_j [1 - \beta(\frac{T_{lj-1} + T_{lj}}{2} - T_0)] - L_j f_l (Q_{l0} - \sum_{k=1}^{j-1} W_{lk}) \} \quad (20)$$

$$p_{ri} - p_0 = \sum_{j=1}^i \{ \rho_0 g L_j [1 - \beta(\frac{T_{rj-1} + T_{rj}}{2} - T_0)] - L_j f_r (Q_{r0} - \sum_{k=1}^{j-1} W_{rk}) \} \quad (21)$$

Mention the fact that the inlet pressure p_0 is the same in both inlets, but also the pressures at the bottom should be the same $p_{ln} = p_{rn}$ and therefore subtracting Eqs.(20-21) for $i=n$ gives the relationship between inlet flowrates in the left and in the right lateral channel

$$0 = \sum_{j=1}^n \{ -\rho_0 g L_j \beta (\frac{T_{lj-1} + T_{lj} - T_{rj-1} - T_{rj}}{2}) - L_j [f_l (Q_{l0} - \sum_{k=1}^{j-1} W_{lk}) - f_r (Q_{r0} - \sum_{k=1}^{j-1} W_{rk})] \} \quad (22)$$

or rearranging terms

$$\frac{\rho_0 g \beta}{2} \sum_{j=1}^n L_j (T_{lj-1} + T_{lj} - T_{rj-1} - T_{rj}) = L (f_r Q_{r0} - f_l Q_{l0}) + \sum_{j=1}^n L_j \sum_{k=1}^{j-1} (f_l W_{lk} - f_r W_{rk}) \quad (23)$$

In the case that geometry of both lateral channels is the same, the Eq.(23) can be expressed in the form

$$\frac{\rho_0 g \beta}{2} \sum_{j=1}^n L_j (T_{lj-1} + T_{lj} - T_{rj-1} - T_{rj}) = L f (Q_{c0} - 2Q_{l0}) + f \sum_{j=1}^n L_j \sum_{k=1}^{j-1} (W_{lk} - W_{rk}) \quad (24)$$

This is not surprising, that Eq.(23) reduces to Eq.(7) in the case without crossflow ($W=0$). However it is not so easy to use this equation as an analytical solution for a general values L_i and general crossflow W_{li} . The crossflow is related to the pressure differences between lateral and central channels. When calculating friction coefficient f_w the two components are considered: Pressure drop corresponding to viscous forces calculated according to (19) (coefficient f_w) and pressure drop corresponding to acceleration of liquid (Borda's losses):

$$p_{li} - p_{ci} = \frac{\rho W_{li}^2}{2(Bh)^2} + f_w W_{li} \quad (25)$$

$$p_{ri} - p_{ci} = \frac{\rho W_{ri}^2}{2(Bh)^2} + f_w W_{ri} \quad (26)$$

These quadratic equations enable to express the flowrate as a function of pressure differences

$$W_{li} = \frac{(Bh)^2}{\rho} \left(-f_w + \sqrt{f_w^2 + \frac{2\rho(p_{li} - p_{ci})}{(Bh)^2}} \right) \quad (27)$$

$$W_{ri} = \frac{(Bh)^2}{\rho} \left(-f_w + \sqrt{f_w^2 + \frac{2\rho(p_{ri} - p_{ci})}{(Bh)^2}} \right) \quad (28)$$

Iterative solution can be as follows:

1. Flowrates at inlet (or ratio of flowrates Q_{i0}/Q_{c0}) are selected as an initial approximation. Cross-flow W_{li} W_{ri} is also estimated, for example as zero.
2. Flowrates in cells are calculated from continuity equations (10-11)
3. Knowing flowrates the complete temperature profiles are calculated from (12-14)
4. Pressures are calculated from Eq.(20-21) and (25-26), giving improved values of cross-flow.
5. New ratio of flowrates at inlet is calculated from Eq.(24).
6. Continue next iteration starting at step 2.

This integral model forms a basis for development of spatially localised RTD (Residence Time Distribution) model. Each cell in Fig.3 is described by subsystem of NC ideally mixed tanks, and flow-rates at inlets to these subsystems (including cross-flows) are given by preceding analysis. Thus it is possible to describe the spatial distribution of concentration of tracer as a function of time. Initial conditions (concentration of trace inside the heater) is zero, and inlet concentration at entry to lateral channels can be an arbitrary function of time (delta function or experimentally determined stimulus function). Resulting system of ordinary differential equations is integrated numerically.

It is true that approximation of tracer dispersion in convective laminar flow by a model formed by ideally mixed tanks is rather crude and cannot properly describe details of flow near walls. However, the model is simple and comparison with experiments indicates that the errors of calculated residence times are acceptable.

Algorithm is implemented in CVASYM.FOR

5. Results of numerical simulations

It is possible to obtain two different solutions for the flow and temperature field taking the effect of natural convection into account:

- Symmetric solution (flowrates in lateral channels equal and temperatures at the two lateral channels are the same). This symmetric regime is stable in the sense, that disturbances are damped.
- Asymmetric solution exists only within a certain range of operational parameters (flowrates and heating power / voltage). This solution predicts different flowrates and temperatures in lateral channels. However this solution is not stable and represents in fact only a stability limit of the symmetric flow.

The following Fig.4 demonstrates that this asymmetry could appear at voltage 30V if the lateral channel is wide (2.2 cm), at 60V for 1.5cm, and 100V if the channels are narrow (1 cm). Values of ratio Q_l/Q (flowrate in left channel / total flowrate) at higher voltage (and therefore more intensive heating) can be interpreted as the flow asymmetry disturbance which is necessary for the existence of this second asymmetric solution.

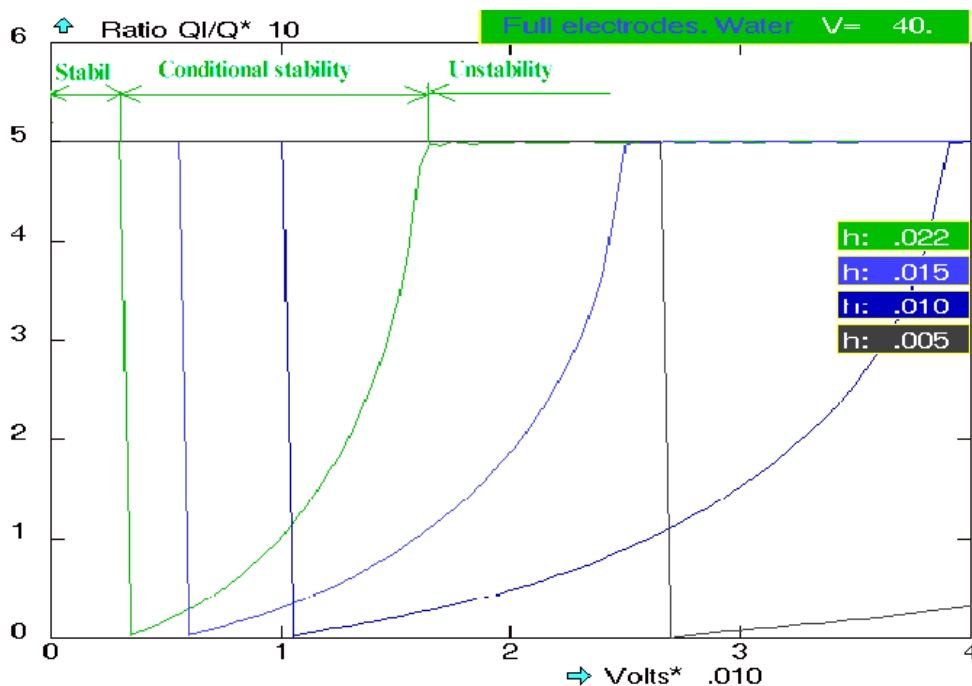


Fig.4 Water $\mu=0.001$ Pa.s, $\beta=0.5 \cdot 10^{-3}$ K^{-1} , $a=0.15 \cdot 10^{-6}$ m^2/s , $\kappa_0=0.0223$ S/m, $\kappa_1=0.0009$ S/(m.K), $c=4200$ J/(kg.K), full electrodes, flowrate 40 ml/s. Different thickness of lateral channels $h_1=0.022, 0.015, 0.01, 0.005$.

Similar graphs can be calculated for other materials, differing first of all by viscosity. Stability problems are even more pronounced for example when heating whole milk (viscosity at 70°C is lower, approximately 0,0006 Pa.s), while sweet cream with the fat content has viscosity higher, approximately 0.004 Pa.s, and condensed non-sweetened exhibits viscosity within the broad range from 0.015 to 0.5 Pa.s, see Houška 1994. Figs.5 is calculated for the same parameters as in Fig.4 but for viscosity 2 mPa.s. It is seen that the stability of flow is increased considerably.

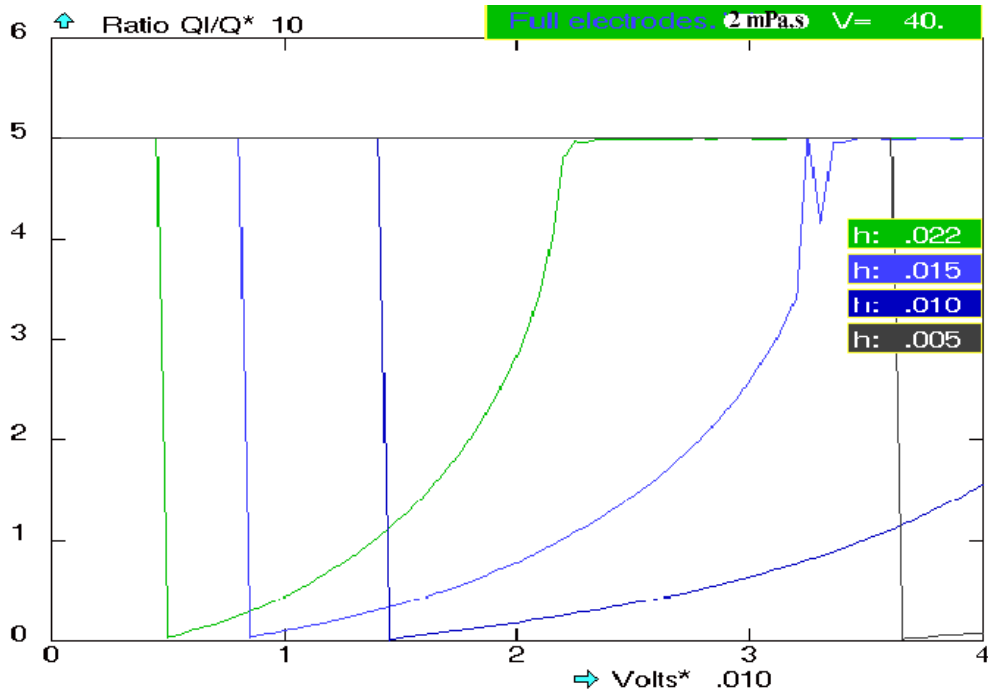


Fig.5 $\mu=0.002$ Pa.s, $\beta=0.5 \cdot 10^{-3}$ K⁻¹, $a=0.15 \cdot 10^{-6}$ m²/s, $\kappa_0=0.0223$ S/m, $\kappa_1=0.0009$ S/(m.K), $c=4200$ J/(kg.K), full electrodes, flowrate 40 ml/s. Different thickness of lateral channels $h_l=0.022, 0.015, 0.01, 0.005$.

The effect of natural convection onto cross-flow through perforated electrodes is demonstrated in Figs. 6 and 7

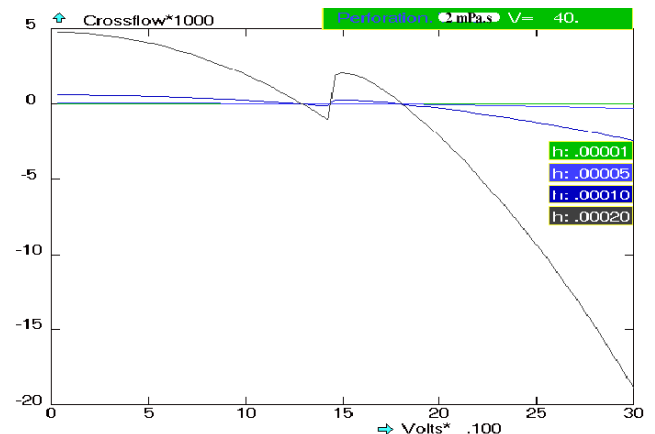
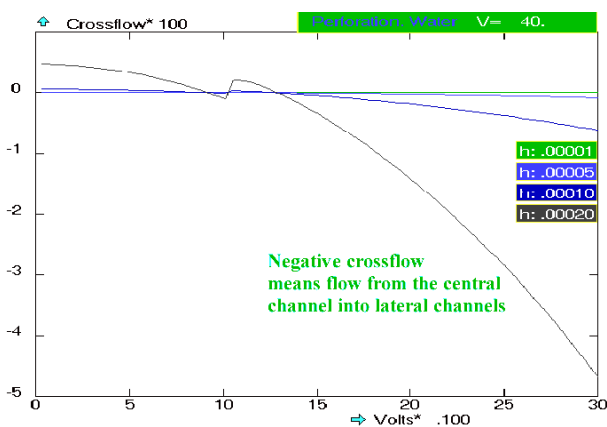


Fig.6,7 Overall crossflow as a function of voltage and width of perforation.

The following figures illustrate behaviour of ohmic heater using residence time distributions

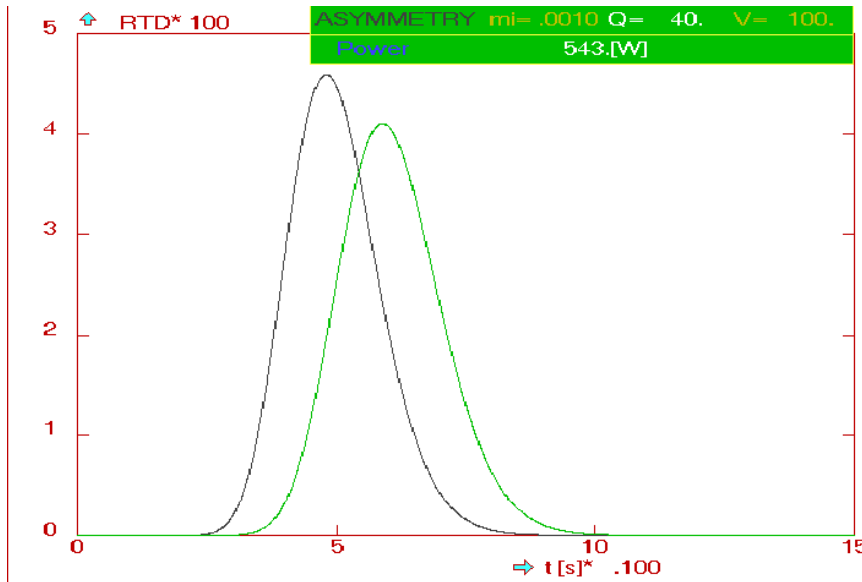


Fig.8 Effect of ASYMMETRY without heating and for full electrodes

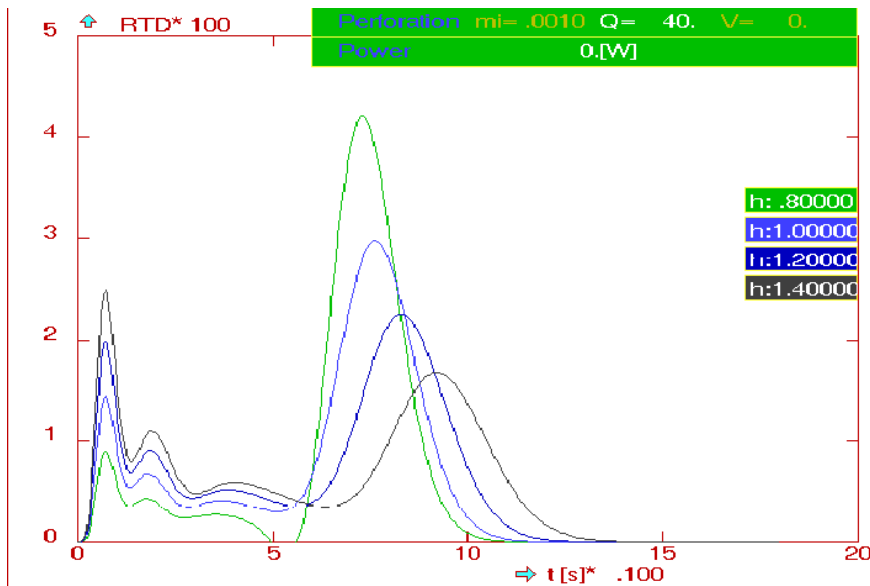


Fig.9 Effect of heating: high cross-flow at constant temperature

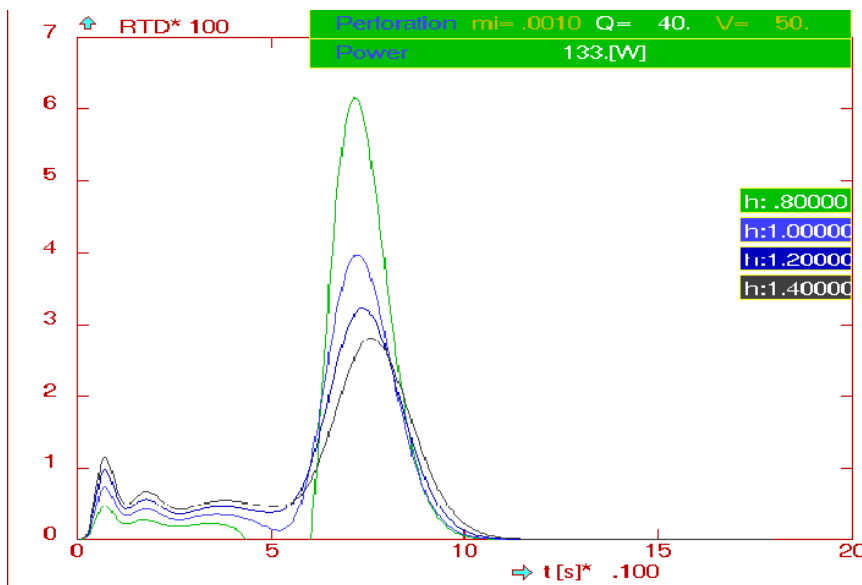


Fig.10 Effect of heating: suppressed cross-flow at heating

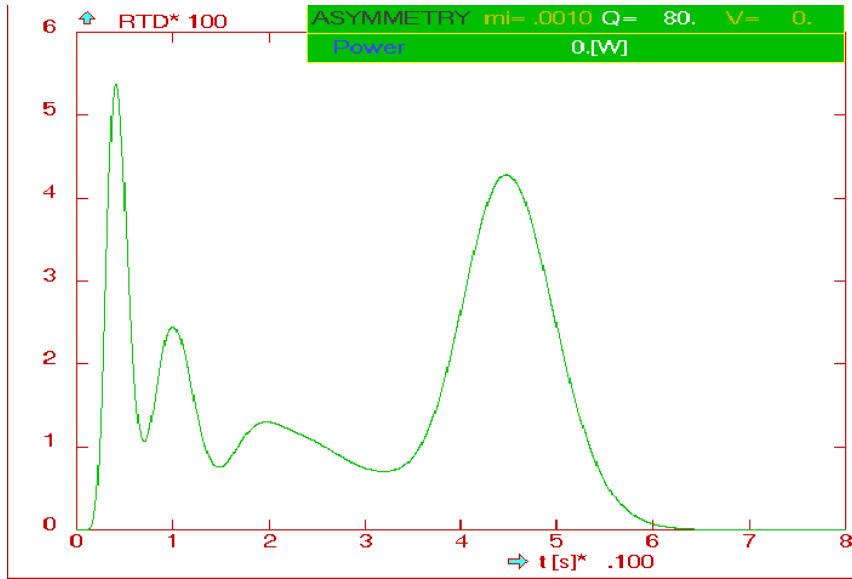


Fig.11 Effect of width of lateral channels: Cross-flow high in narrow channel ($h_1=0.01\text{m}$)

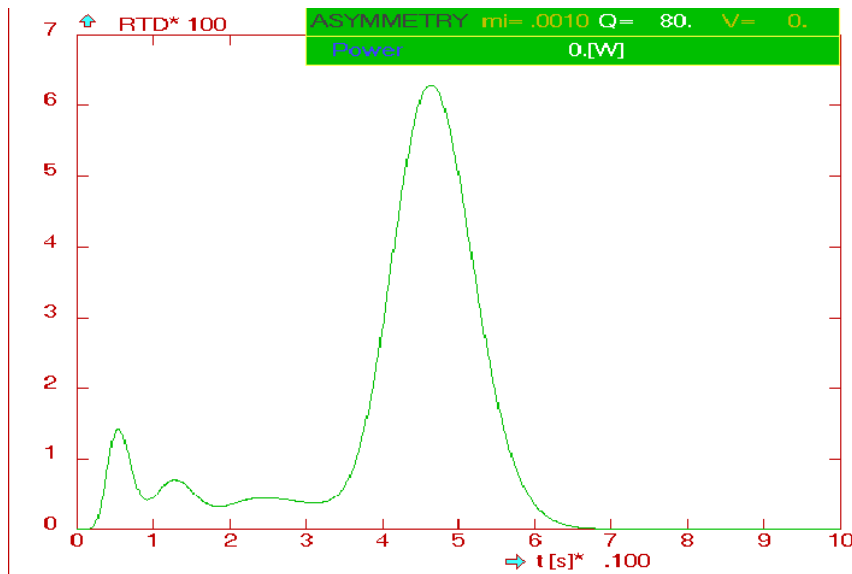
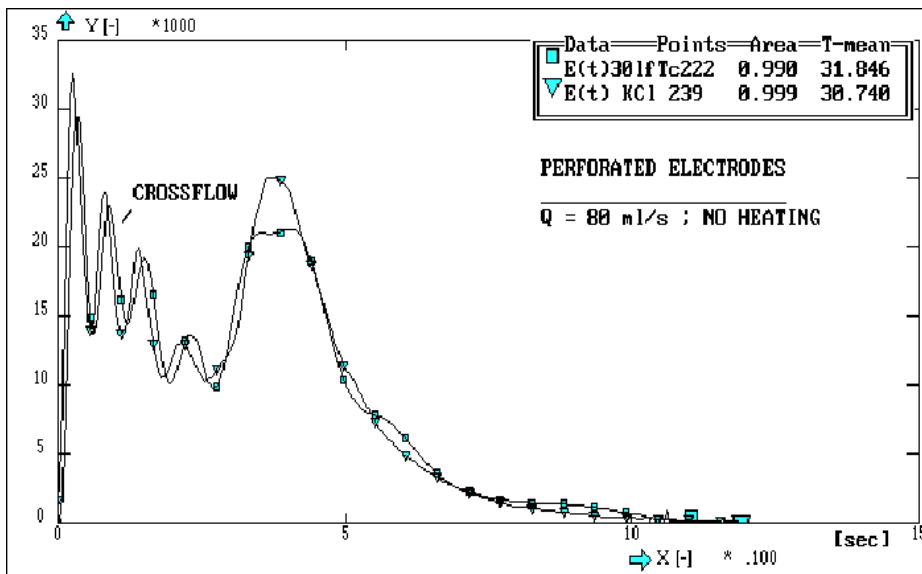


Fig.12 Effect of width of lateral channels: Cross-flow is low in wide channel ($h_1=0.02\text{m}$)

6. Experiments

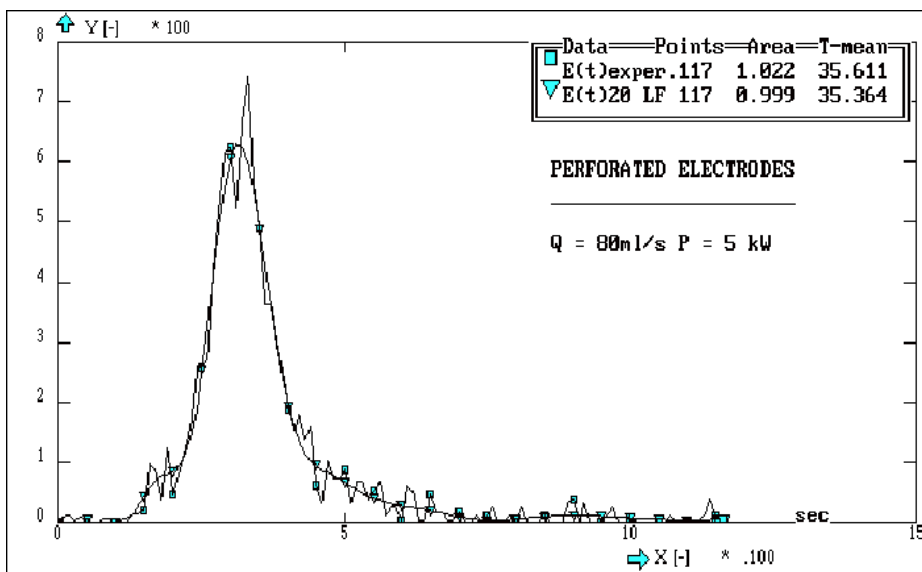
Experiments were performed with different thickness of lateral channels (22 mm and 12 mm). Temperature at lateral channels was recorded by two Pt100 probes which prove to be a sensitive indicator of flow instabilities. Residence time distribution was identified by using KCl and Tc-99 as a tracer. Results obtained with these tracers are very similar, however the radioisotope is a better tracer at heating because Tc99 has no effect upon direct ohmic heating (this is not true for KCl which increases power and temperature when passing between electrodes).

Selected results are shown in Figs. 13 and 14



00E0PLFV.R1

Fig.13 Comparison of conductivity and radioisotope methods



00ER5P1

Fig.14 Perforated electrodes – heating suppressed cross-flow

7. Conclusions

The asymmetry of flow can be suppressed by

- Decreasing the width of lateral channels (this is the most efficient way)
- Increasing viscosity (it has similar effect, pressure drop in lateral channels must be more important, than the change of density)

- Cross-flow (perforation) has also positive effect improving stability, however this is not very significant.

References

1. Houska: Milk, milk products and semiproducts, Prague, 1994
2. Kays W.M., Crawford M.E. : Convective Heat and Mass transfer, McGraw Hill, 1993
3. Novák V., Rieger F., Vavro K.: Hydraulické pochody v chemickém a potravinářském průmyslu, SNTL Praha 1989
4. Thýn, J., Žitný, R., Computer Fluid Dynamics and Tracer experiments, CVUT Workshop 2000, Praha, 14-16 February (2000)
(<http://workshop.cvut.cz>)
5. Žitný, R., Thýn, J., Verification of CFD predictions by Tracer Experiments, International Conference CHISA 2000, Prague, 28 - 31 August (2000) .